POAC'23
Glasgow, UK

Proceedings of the 27th International Conference on
Port and Ocean Engineering under Arctic Conditions
12-16 June 2023, Glasgow, United Kingdom

Comparison of sequential and coupled approaches for dynamic ice loads by regime extent analysis

Victor Granlund[1], Björn Schümann[1], Jeffrey Hoek[2]
[1]Ramboll, Hamburg, Germany
[2]Siemens Gamesa Renewable Energy, The Hague, Netherlands

ABSTRACT

The calculation of dynamic level ice loads on vertically-sided offshore wind turbine foundations using industry-standard models is complex, with significant interplay between aeroelastic loads, turbine and support structure dynamics and ice action. The ice model VANILLA has features including contact area variation, strain-rate dependent strength, and nonlinear contact and breakage events. The resulting ice-structure interaction is sensitive to changes in the dynamic properties of the turbine and support structure, which in turn depend on the operating conditions at any point in time. Due to the multitude of operating variables and the nondeterministic nature of the load model, the resulting regime of ice-structure interaction is difficult to predict. Insight into the interaction processes must come from careful analysis of time domain results.

This paper evaluates the differences between two model setups, where one is sequential and the other is fully-coupled. In the sequential setup, the public domain VANILLA solver is used to calculate a "pre-defined" ice load time series based on a modal representation of the turbine and the support structure, and this load time series is used as input in an aeroelastic simulation. In the fully-coupled setup, VANILLA is used to calculate ice loads simultaneously to wind loads within an aeroelastic solver. The fully-coupled method requires careful integration of the sea ice model into the aeroelastic solver, while programs for calculating ice loads sequentially presently exist in the public domain. Differences in the output from the two setups is presented and discussed.

A regime classification algorithm is presented and applied to compare the results from each setup. The classification algorithm quantifies the amount of intermittent crushing or frequency lock-in within a time series, so that a systematic analysis can be performed when a wide range of operating conditions is simulated and the amount of output data is large. The results of the classification reveal at which ice velocities the interaction regime changes under any set of operating conditions. The viability of the sequential setup as an engineering method is demonstrated.

KEY WORDS: Ice-induced vibrations; Offshore wind turbines; VANILLA; Linearisation; Regime classification.

NOMENCLATURE

BHawC	: SGRE's in-house aeroelastic software package.
CBC	: Continuous brittle crushing
DLC	: Design Load Case
FLI	: Frequency lock-in
FLS	: Fatigue Limit State
IC	: Intermittent crushing
IIV	: Ice-induced vibrations
LTI	: Linear time-invariant
SGRE	: Siemens Gamesa Renewable Energy.
ULS	: Ultimate Limit State
VANILLA	: Variation of contact Area model for Numerical Ice Load Level Analyses.

INTRODUCTION

Level ice loads can have a significant impact on the structural design and performance of offshore structures, and accurately simulating these loads is crucial for safe and cost-effective design. However, the complexity of the ice-structure interaction and the interplay between aeroelastic loads, turbine dynamics, and ice action make it difficult to predict the dynamic response, setting a high precedent for software integration.

It can be difficult to motivate the significant software integration costs, especially for projects in sites where ice conditions are not severe or where the ice season is very short. In such cases, self-contained solvers that work using a simplified modal domain representation of the global structural dynamics can provide a simpler and more cost-effective solution. Such a model typically uses the results of a natural frequency analysis to provide the modal frequencies, displacements, and damping values. The performance of a sequentially calculated dynamic load time series based on a modal domain linear time-invariant model is dependent on the similarity of the linearization to the full aeroelastic model.

Non-coupled dynamic load calculation can be expected to produce poor results if the linearization is a poor representation of the full dynamic system. Possible error caused by structural model dissimilarity is evaluated by looking at the similarity of the resulting waterline deflections from the detached solver (Public domain VANILLA solver in combination with linearized structure) to the deflections caused in the full aeroelastic model when the same (*sequential*) load time series is applied therein. Any amplification or cancellation of dynamics is unwanted.

Secondly, the applicability of a modal domain LTI model for calculating ice loads on an offshore wind turbine may be investigated by comparing the sequentially achieved results with the fully-coupled results. This is done to ensure that there are no significant effects that are not captured when using a linear modal domain representation of the structure.

This paper aims to demonstrate the application of such a model, which is available in the public domain (Hendrikse, 2018), and to highlight the necessary considerations and potential risks associated with this approach. The results of sequentially calculated loads are compared to the results of a fully-coupled simulation, and the data is systematically analyzed to evaluate the similarity of both methods. By doing so, this paper aims to provide insight into how simpler models can be used to simulate sea ice loads, and to contribute to the development of more effective and efficient design methods for offshore structures.

METHODS

The method section is structured into four components, providing a detailed account of the tools utilized for conducting the analysis and postprocessing the results.

VANILLA

VANILLA is an industry-standard model for representing dynamic ice loads, which has been developed at TU Delft. The most recent version of the model has can be found on Mendeley (Hendrikse & Nord, 2019). The model discretizes the contact between a vertically-sided offshore structure and a continuous level ice sheet, moving at a uniform rate towards the structure. The ice sheet is partitioned into N independent elements, each consisting of a system of nonlinear springs and dampers, which simulate the stress-rate dependent resistance to compression of level ice, see Figure 1. The failure criterion of an ice element facilitates a brittle failure under a rapid stress rate, and a ductile, stronger failure under a moderate stress rate.

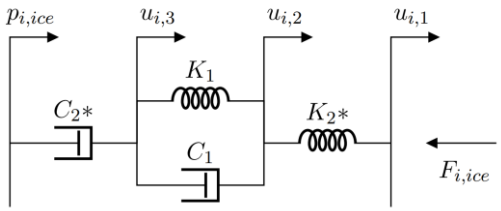

Figure 1: A depiction of the parts of an ice element.

As these elements react to structural compliance and vibrations, they recreate the load and contact area variation trends that have been measured in empirical test campaigns. After each failure of an ice element, the model reintroduces an ice element at a short distance from the structure to keep the number of ice elements in the simulation constant.

The simplified material model used to capture the effects of crushing events on semi-rigid structures is defined by 7 internal parameters, which are tuned to match full-scale data. Through this process, the model is designed to phenomenologically emulate the behaviour observed in real structures. The statistical properties of the load trends against a rigid structure are analytically described and used to relate the model behaviour to empirical data. Some general trends of VANILLA can be seen in Figure 2. Additionally, the statistical properties are utilized to scale the model behaviour to different ice thicknesses and structural dimensions. The methods do not require users to be familiar with the empirical data as the full-scale data can be related to formulas in ISO19906:2019 (ISO, 2019).

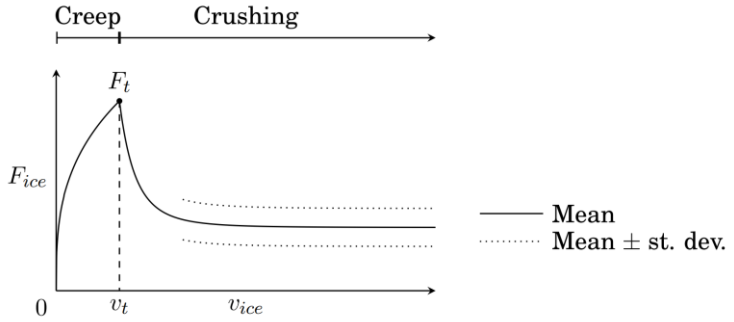

Figure 2: The general ice load trend as a function of ice velocity in VANILLA.

In the coupled analysis, the simulation is performed entirely in BHawC, where VANILLA has been integrated (Willems & Hendrikse, 2019). In the sequential method, the ice load was calculated using the public domain model and reapplied as a node load in BHawC.

Turbine model, support structure and site conditions

The wind turbine model used in this study is an SGRE turbine with a rated power of 15 MW and a rotor diameter of 236 m. The operational wind speed ranges from 4 m/s (cut-in) to 28 m/s (cut-out) and the rated power is reached for a wind speed of 12 m/s. The turbine and tower structure are supported by a monopile foundation in 37.5 m water depth. The width at the waterline is 7.5 m. Linearized soil-structure-interaction curves were used, as this decreases the potential mismatch between dynamic linearisation and full model. The natural frequencies of the 1st, 2nd, and 3rd fore-aft global bending modes of the integrated structure are 0.145 Hz, 0.79 Hz, and 1.77 Hz respectively.

In this study, two ULS DLCs according to (IEC, 2019) have been considered: DLC D3 (power production) and DLC D8 (parked/idling conditions). The D3 ice-structure interaction simulations are performed at a windspeed of 12 m/s (hub height), while 1 m/s was used for D8. D3 was split into an aligned case, where the ice and wind are acting in the same direction (turbine fore-aft), as well as a misalignment case of 90 degrees, where the wind acts perpendicular to the direction of the ice load. The misaligned case is denoted as D3_M. No yaw error was considered, as the effect of yaw error on the properties of the linearisation is not strong.

Three ice thicknesses were simulated, 0.15 m, 0.25 m, and 0.35 m. All thicknesses were simulated at a range of ice drift velocities from 0.01 m/s to 0.13 m/s with increments of 0.01 m/s. An ice strength coefficient C_R of 1.0 MPa has been considered.

Linearisations

A linearisation of the global structural dynamics is necessary as an input for the public domain VANILLA solver. When creating a linearization, there are several properties that must be accounted for:

- The static stiffness/compliance of the structure.
- The mode shapes, considering the amplitude of the mode at the ice action point, which is correlated to the excitability of a specific mode to a force at this elevation.
- The damping of each mode. A significant part of the damping in a wind turbine comes from aerodynamic rotor damping, which will change with the rotor pitch and wind velocity. Thus, wind speed dependency cannot be entirely neglected.
- Like damping, modal shapes and frequencies also change with rotor pitch.
- Other variables that may affect the dynamics:
    - Yaw error
    - Water level
    - Corrosion & marine growth presence
    - Soil stiffness (degradation)

One clear drawback of the sequential method is the management necessary to handle the large amount of linearisation data required for a typical load case table as per IEC61400-3-1 (IEC, 2019). The correct linearisation needs to be chosen for each simulation, and all linearisations must be updated when significant changes are made in e.g. the turbine or the foundation. The feasibility of such a workflow may depend on how time consuming the linearisation process is, and how many technical stakeholders are involved. If the foundation is represented by a superelement, the turbine vendor/the linearizing party may need to transfer data to the foundation designer in order for a superelement expansion to take place, yielding the displacement at waterline.

In addition to modal frequencies and damping ratios, the public domain VANILLA solver shall receive mass-normalized modal amplitudes at the ice action point. Together these form the structural input to the solver.

The eigenanalysis of a damped system like a wind turbine results in complex eigenvectors. The correct treatment of these eigenvectors is crucial to achieving accurate results, and the presence of a phase irregularity in the mode shape is something that the VANILLA solver cannot account for. If dynamic loads were calculated on multiple parts of the structure at once, there may exist a phase difference between two nodes within a mode, and this cannot be accurately represented with this solver. There may be significant phase difference between e.g. the rotor and the ice action point, which indicates that inserting wind loads in such a solver may lead to erroneous results. In this paper, the only load applied in the VANILLA solver is the VANILLA ice load.

One example of how the properties of a linearisation depend on the environmental operating conditions as well as details on how linearisations can be created are found in (Augustyn, et al., 2022).

Classification algorithm

As already mentioned, the interaction of level ice and vertically-sided structures, such as a monopile, is a complex dynamic and highly non-linear process. The ice's strength, thickness, and drift velocity in combination with the dynamic properties of the structure may result in three different failure regimes of the ice: intermittent crushing, frequency lock-in and continuous brittle crushing. These failure regimes have distinct characteristics in terms of global ice load and structural response, see Figure 3 and Figure 4.

Intermittent crushing occurs at low ice speeds and is characterized by a saw-tooth pattern in both the structural displacement and global ice load. The frequency is smaller than or equal to the first natural frequency of the structure. Frequency lock-in can develop at intermediate speeds and in this regime, the ice failure is periodic with a period equal to one of the natural periods of the structure. The structural response is characterized by an almost harmonic response, where the maximum structural velocity in the direction of the ice drift lies between 0.8 and 1.5 times the ice drift speed. Both intermittent crushing and frequency lock-in can contribute significantly to the fatigue of a structure, depending on the probability of the condition in which they occur. The response amplitudes are higher in intermittent crushing compared to the frequency lock-in, while the frequency is lower.

The last regime is continuous brittle crushing, which develops for high ice speeds or when the structure is sufficiently stiff or damped to prevent the other two regimes from occurring. In this regime the ice load is aperiodic, independent of the structural motion and smaller in magnitude compared to the other two regimes, making it least critical for the structure.

In this paper, we introduce an algorithmic method for classifying the interaction regime, which is utilized by Ramboll for data exploration and quantitative insight into time series results. This method is helpful in demonstrating the coverage of relevant interaction velocities in a load case table and identifying ice velocities that may result in peak response. In this paper, we apply the algorithm to explore the differences in regime velocity boundaries when comparing fully-coupled to sequentially calculated ice-structure interaction.

The input to the algorithm is the displacement time series at the ice action point, measured in the direction of ice travel, and the ice velocity. No information about the modal properties of the structure is required.

The normalized velocity vector v_N is calculated as the numerical time derivative of the deflection time series normalized by the ice velocity. Next, the derivative of the normalized velocity vector is calculated and denoted v'_N.

In order to identify which regime is occurring in the time series, a couple of conditions will be applied to the vectors. The intersections of the Boolean vectors allow to identify specific patterns in the time series.

Intermittent crushing is signified by a period of stable load build-up, where the structure is slowly deformed until the ice fails. The following transient spring-back is typically much shorter than the duration of the build-up. During the build-up phase, the structure experiences stable positive velocity in the same range as the ice velocity, and low accelerations.

The following criteria have been found to work well to identify IC:

$$0.2 < v_N < 2 \quad (1)$$

$$|v'_N| < 0.3 * avg(|v'_N(v'_N < 0)|) \quad (2)$$

The quantity $avg(|v'_N(v'_N < 0)|)$ represents the average absolute accelerations during the transient phase of the IC cycle. There may be other criteria that work equally well, and the coefficient of 0.3 has been tuned by visually inspecting the applicability of the criteria to various time series data.

The union of the Boolean vectors resulting from applying the two criteria is denoted B_{IC}. The average truth over B_{IC} is calculated, and the resulting scalar represents the ratio of timestep data within the time series that fulfils both criteria. This value is less than 1, even in a time series where only IC occurs.

It has been observed that the maximum structural velocity during a cycle of FLI often falls between 0.8 and 1.5 times the ice velocity (Hendrikse & Nord, 2019). For identifying FLI, a single criterion is applied such that

$$B_{FLI} = 0.8 < |v'_N| < 1.5 \quad (3)$$

The average truth over B_{FLI} is less than one for a time series where only FLI occurs. This is because there are phases of the harmonic vibration where the velocity is 0.

There is usually significant overlap between the vectors B_{FLI} and B_{IC}, which would indicate that both regimes occur in the same timesteps. The average Boolean truth of each vector is also always below 1. There may also sometimes be noise, where some part of the time series that is clearly not FLI is misidentified as FLI. All these considerations are dealt with in the next step,

where C_{IC} is calculated. C_{IC} is the content of IC within the time series.

$$C_{IC} = \mathrm{a_{time}} avg(B_{IC}) - \mathrm{a_{noise}} \quad 4.$$

If C_{IC} is less than 0, it is substituted by 0. If it is above 1, the result is substituted by 1. a_{time} is found by inspecting a time series of IC and measuring the ratio of the duration of the build-up phase to the duration of the complete cycle. $\mathrm{a_{time}}$= 1.69 is appropriate. $\mathrm{a_{noise}}$ is necessary because the IC criteria may sometimes be true for a short phase of a FLI time series. $\mathrm{a_{noise}}$= 0.15 is appropriate.

$$C_{FLI} = \mathrm{b_{time}} avg(B_{FLI}) - C_{IC} - \mathrm{b_{noise}} \quad 5.$$

The same clipping to [0, 1] is done for C_{FLI}. The factor $\mathrm{b_{time}}$ has been tuned by measuring what part of a typical harmonic FLI pattern fulfils the criteria, and $\mathrm{b_{time}}$= 2.6 has been found to be appropriate. $\mathrm{b_{noise}}$= 0 has been found to be appropriate, but may lead to false positives if there is significant wind turbulence.

RESULTS

In Figure 3 and Figure 4, some individual time series results are shown, displaying 60 second spans of ice-action point deflections. The deflection is measured in the direction of ice drift. Above each plot, some information about the simulation conditions is shown (SIMID = simulation ID, ICEVEL = ice velocity [m/s], DLC_NUM = DLC number, WISPEED = wind speed [m/s], MISAL = wind-ice-misalignment [degrees], ICETHI = ice thickness [m]), as well as the algorithmically derived contents of FLI and IC in the 600 second simulations (200 s start-up + 600 s results).

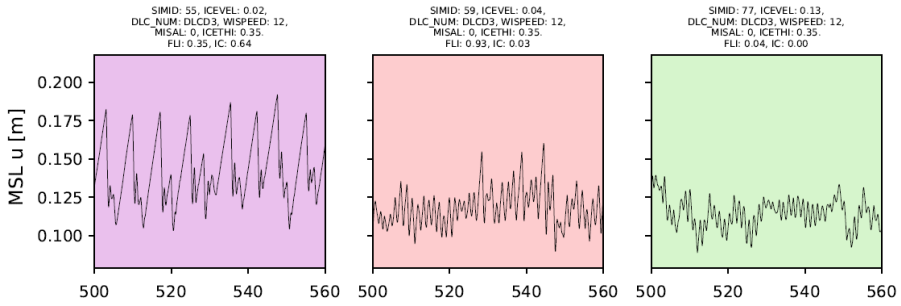

Figure 3: A subset of time, ice action point deflection plots from the coupled D3 results, where the time series background has been coloured by the algorithmically identified regime contents (Blue: IC, Red: FLI, Green: CBC).

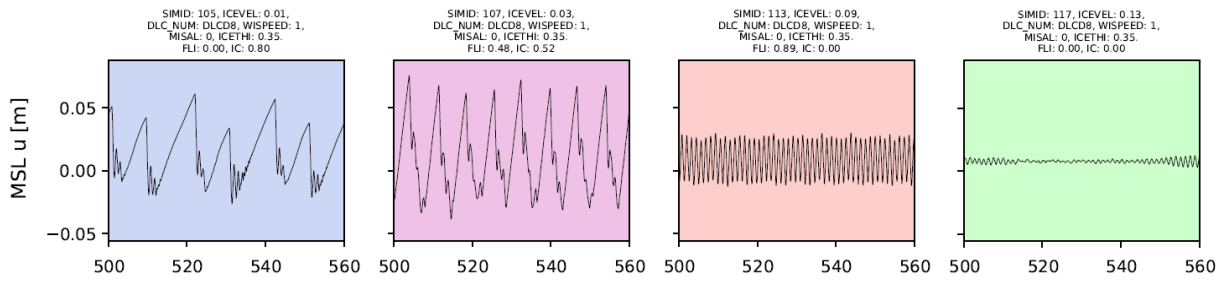

Figure 4: A subset of time, ice action point deflection plots from the coupled D8 results, where the time series background has been coloured by the algorithmically identified regime contents (Blue: IC, Red: FLI, Green: CBC).

In Figure 5, Figure 6 and Figure 7, the regime boundaries are presented for each combination of ice velocity (ICEVEL [m/s]) and ice thickness (ICETHI [m]). The colour scheme is the same as seen in the background of Figure 3 and Figure 4.

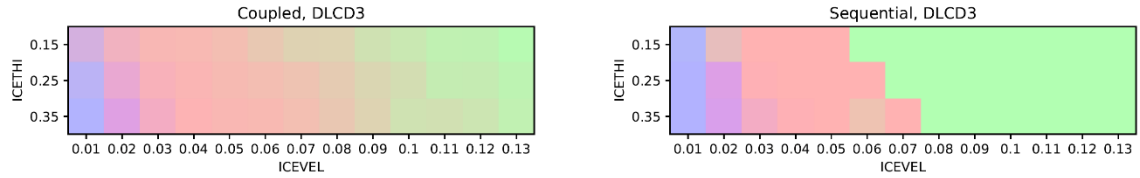

Figure 5: Comparison of regime boundaries in DLC D3 for the coupled (left) and sequential (right) approach.

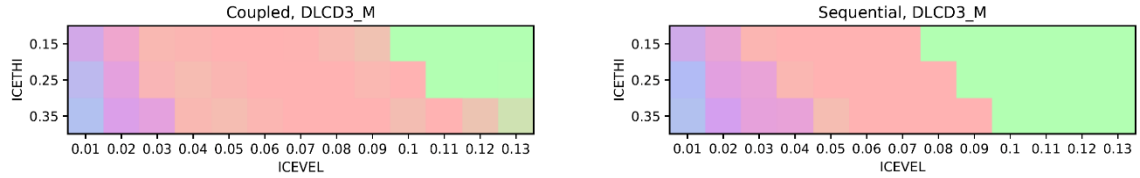

Figure 6: Comparison of regime boundaries in D3 with misalignment for the coupled (left) and sequential (right) approach.

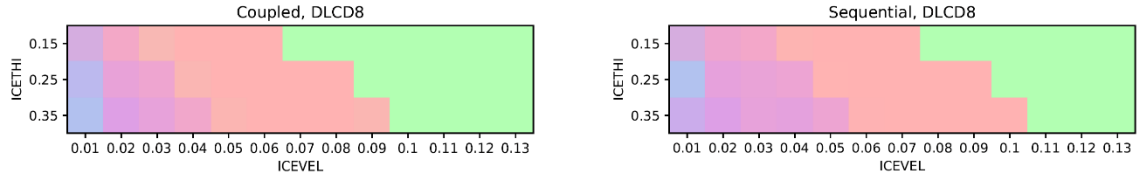

Figure 7: Comparison of regime boundaries in D8 for the coupled (left) and sequential (right) approach.

Some mismatch in transition velocities is observed in all DLCs, likely related to linearisation inaccuracy. Blurring of the transition is observed in the coupled DLC D3 results, which is caused by turbulence. The differences are further discussed in the Discussion section. A finer load case table and seed-averaged results would be needed to quantify the exact mismatch.

ULS load envelopes

The sequential results were postprocessed by evaluating the resulting maximum horizontal bending moment along the foundation structure, in groups of different ice thicknesses within DLC D3. These load envelopes were normalized by the corresponding envelopes for the coupled results. In this way, we can quantify the error introduced by the sequential load calculation method in relative terms, and such results are illustrated in Figure 8.

The bending moments were extracted at elevations +10 m (Foundation-tower interface), 0 m (Waterline), −9.4 m, −18.8 m, −28.1 m, and −37.5 m (Mudline). The plots in Figure 8 were smoothed using spline interpolation.

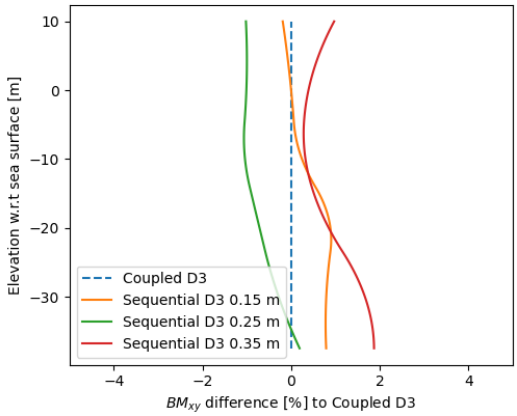

Figure 8: Relative difference in horizontal bending moment between the sequential and coupled results, shown for three different ice thicknesses.

The difference shows no clear trend w.r.t. ice thickness. It is expected that the envelope match would further improve with seed averaging, which would always be applied in a project setting.

Sequential results – Detached solver vs aeroelastic simulation

As the validity of the result is contingent on the similarity of the linearisation to the dynamic behaviour of the full model, the similarity must be evaluated. For an ideal linearisation, there would be no change in the amplitude or shape of ice-induced response when the forces from the detached solution are reapplied in the aeroelastic simulation. Thus, the success of the simulation can be gauged by comparing the similarity of displacement patterns at waterline between the detached solver and subsequent aeroelastic simulation.

Such a comparison is shown in Figure 9: Comparison of ice induced vibrations in the detached solver (yellow) to the behaviour of the full model (black) in D3.Figure 9 and Figure 10, and it is seen that in D3, the match is good, indicating that the linearisation was an effective representation of the full model. However, in D3_M (not shown) and in D8 (Figure 10), similarity was poor in some conditions, indicating that the linearisation process needs adjustment.

Note that some mismatch is caused by turbulence and wind thrust, which are not present in the detached solver. The deflection data must be mean-value corrected, so that the ice-induced vibration amplitudes can be compared. In Figure 9, SIMID 59, the mismatch is caused mostly by turbulence effects.

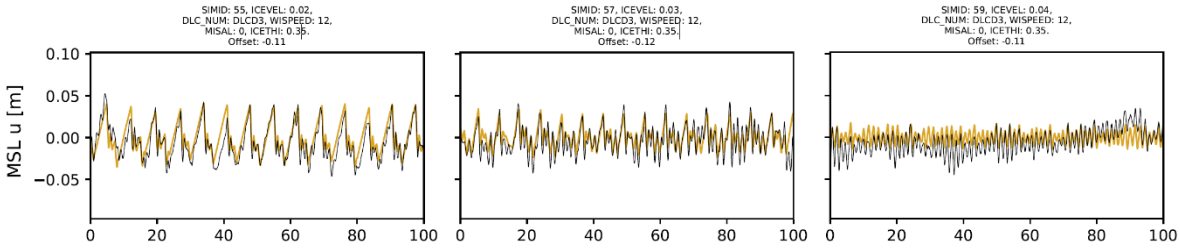

Figure 9: Comparison of ice induced vibrations in the detached solver (yellow) to the behaviour of the full model (black) in D3. Left and centre: IC, right: FLI.

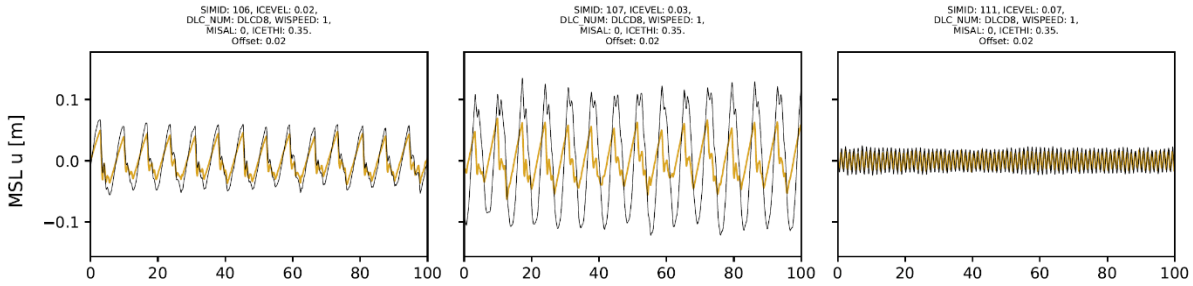

Figure 10: Comparison of ice induced vibrations in the detached solver (yellow) to the behaviour of the full model (black) in D8. Left and centre: IC, right: FLI.

The cycle of iterating on the linearisation process based on time series results can be slow. The results shown in this paper are based on linearisations as provided by BHawC with no modification, and the authors have not performed any iteration of the linearisation process to arrive at these results.

Coupled vs. Sequential results

Comparing the output of the sequential and coupled methods directly may also yield valuable insights. The simulations share the same turbulence seed, allowing us to isolate which vibrations are related to turbulence, as opposed to being ice-induced. Because the ice was simulated completely independently, any similarity between the two in e.g. the phase in IC is completely random. A comparison of a subset of simulations in D3 is shown in Figure 11.

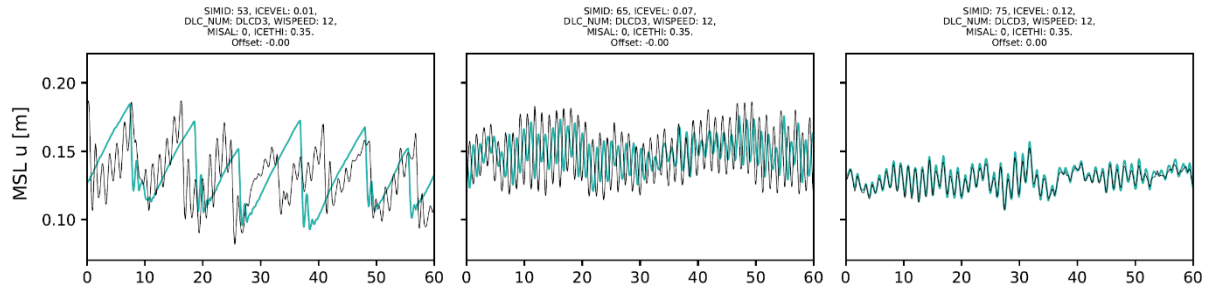

Figure 11: Comparison of deflection time series of the coupled simulation (teal) to the sequential simulation (black) in D3. Left: IC, centre: FLI, right: CBC.

Several observations can be made from our analysis. Firstly, we note that the durations of IC-

cycles appear to be more irregular in the coupled simulation. This is likely because turbulence can either extend or prematurely interrupt a cycle of IC. Similarly, the prevalence of FLI also seems to be affected by turbulence in the coupled simulation.

According to our previous definitions, accelerations remain low during the loading phase of intermittent crushing. This is not observed in the sequential results. This is because the introduction of turbulence occurs after the ice load simulation has completed, meaning that the ice cannot react to these excitations. Consequently, the confining effect of the ice on excitations from turbulence is not captured. To address this, the regime boundary plots presented in the Results section were performed on the output of the detached solver, and not on the final time series results.

It is difficult to draw definite conclusions on the accuracy of the linearisations based on the visualization in Figure 11, however it highlights which effects are not captured in the sequential load calculation method.

DISCUSSION

The regime boundaries in terms of ice velocity are much more clearly defined in the sequential results. The effective blurring of the transition speed is attributable to the random excitations from turbulence, excitations to which the ice will react in the coupled simulation. In a sequential simulation, the excitations caused by the ice may influence the loads on the rotor, but not vice-versa. For a ULS analysis, the loads during the FLI-CBC transition are usually not critical, as the maximum response usually occurs in the IC-FLI transition velocity. However, the clear boundary between FLI and CBC affects the sensitivity to FLS drift speed distributions. Thus, the sequential method as such is less suitable for locations where the ice season is long, and FLS damage due to ice may be significant.

A larger number of seeds would be required to properly conclude that e.g. the maximum ULS mudline moments are matching for both methods, but it is SGRE's and Ramboll's experience from projects that a good match can be achieved using the methods described in this paper. The maximum ULS response with both methods occurs at the transition velocity between intermittent crushing and frequency lock-in, where the interaction can be called multi-modal (Hammer, et al., 2022). At this velocity, there appears to be significant first and second mode dynamics within one cycle of intermittent crushing. Interestingly, this behaviour is only seen for the thickest ice simulated in this study. When the sequential method is used, the boundary velocity between IC and FLI is also more clearly defined, and a finer load case table may be necessary to capture the peak response.

The added randomness in the coupled results requires a larger amount of simulation seeds to yield a reliable seed-average of loads, compared to the sequential method which exhibits less seed-to-seed variation.

A large number of linearisations may be required to account for variations in operating conditions. This is especially true for structures that are not symmetric – for example a jacket would require linearisations to be specific to each wind direction considered, which is not the case for a monopile. There are also more steps involved in the sequential process, each of which involves an added risk of mistakes compared to the coupled method. On the other hand, the VANILLA ice model is not necessarily straightforward to implement in software, while many aeroelastic packages may include the functionality to linearize the structural dynamic behaviour.

CONCLUSIONS

The sequential load calculation method for dynamic sea ice loads on offshore wind turbines is a useful engineering tool but requires the designer to be aware of certain limitations outlined in this paper. Further work for improving the methods could include modifications that emulate the random excitations seen in coupled simulations, decreasing the sensitivity to the input ice velocity.

Additionally, it would be ideal if there were public domain solvers available which provided added functionality to aid in the process of validating the similarity of the linearisation to the full model. These tests could be focused on scenarios that are simple to compare with the full model, such as static load application at the ice action point, response to a sinusoidal load signal, or a free-decay test.

REFERENCES

Augustyn, D., Cosack, N. & Ulriksen, M. D., 2022. On the influence of environmental and operational variability on modal parameters of offshore wind support structures.

Hammer, T. C., Owen, C. C., van den Berg, M. & Hendrikse, H., 2022. Classification of Ice-Induced Vibration Regimes of Offshore Wind Turbines. Hamburg, ASME.

Hendrikse, H., 2018. Model for simulation of dynamic ice-structure interaction for vertically sided offshore structures - SDOF MATLAB implementation.
Available at: 10.17632/582m8565dj.1

Hendrikse, H. & Nord, T. S., 2019. Dynamic response of an offshore structure interacting with an ice floe failing in crushing. Marine Structures, Volume 65, pp. 271-290.

IEC 61400-3-1:2019: Wind energy generation systems – Part 3-1: Design requirements for fixed offshore wind turbines. Geneva: IEC.

ISO 19906:2019: Petroleum and natural gas industries – Arctic offshore structures. European Committee for Standardization.

Willems, T. & Hendrikse, H., 2019. Coupled Simulation of Ice-Structure Interaction of Offshore Wind Turbines in Bhawc Using Vanilla. Delft: POAC 2019.